Sedimentologika

Research article

The large-magnitude earthquake potential of an active strike-slip fault system in Lake Poso, Central Sulawesi, Indonesia

Nicolas Tournier[1], Stefano C. Fabbri[1,2], Adrianus Damanik[1,3], Flavio S. Anselmetti[1], Taufan Wiguna[3], Sri Yudawati Cahyarini[3], Hendrik Vogel[1*]

[1] Institute of Geological Sciences & Oeschger Centre for Climate Change Research, University of Bern, Baltzerstrasse 1+3, 3012, Bern, Switzerland
[2] Federal Office of Topography swisstopo, Seftigenstrasse 264, 3084 Wabern, Switzerland
[3] Research Centre for Climate and Atmosphere, National Research and Innovation Agency (BRIN), Indonesia

*corresponding author: Hendrik Vogel (hendrik.vogel@unibe.ch)

doi: 10.57035/journals/sdk.2025.e31.1604

Editors: Suzanne Bull and Siddhi Joshi
Reviewers: Nicolas Waldmann, Kathleen Wils and one anonymous reviewer
Copyediting, layout and production: Jarred C. Llyod, Romain Vaucher and Francyne Bochi do Amarante

Submitted: 03.07.2024
Accepted: 04.08.2025
Published: 28.08.2025

Abstract | Earthquakes along the Ring of Fire are considered among the most destructive on Earth. In Indonesia, 19 earthquakes with a magnitude greater than 7.5 have been recorded in the last 20 years, all causing devastating catastrophes. As witnessed by the 2018 magnitude 7.5 Palu earthquake, extensive areas on the island of Sulawesi are particularly prone to seismic hazards due to the converging Australian, Eurasian, Pacific, and Philippine tectonic plates. However, instrumental records show that extensive areas in the central part of the island appear to be seismically quiet in the last century regarding larger magnitude ≥ 7 earthquakes. Lake sediments are excellent sentinels for environmental changes occurring in its near surroundings, hence they serve as a natural archive for events, including seismicity, thus allowing the investigation of the notion of absence of large-magnitude earthquakes. In 2022, we conducted a geophysical and high-resolution bathymetric survey at Lake Poso to provide insight into seismic activity in Central Sulawesi beyond the instrumental record. The survey allowed us to image large subaquatic slides and lake-bottom offsets, which indicate high-intensity earthquakes, possibly related to the presence of an active local fault system. Our paleoseismological assessment suggests a recurrence of large-magnitude earthquakes every 1600 ± 1450 years over the last 11,000 years. Based on our subsurface observations, the evolution of the tectonic Poso basin indicates that large-magnitude earthquakes are also possible in this region. The consequences of such an event may have devastating consequences for local populations and infrastructures in Sulawesi.

Lay summary | The island of Sulawesi in Indonesia is located at the junction of the Australian, Eurasian, Pacific, and Philippine tectonic plates. These collision zones accumulate stress over time, which can be released suddenly in the form of earthquakes. Particularly strong and devastating earthquakes may take decades to hundreds of years of stress accumulation before they occur. Hence, instrumental and historical records are often insufficiently long for proper seismic hazard evaluation. It is therefore important to study prehistoric earthquakes (paleoseismology) and determine the time of occurrence of past events to estimate recurrence probabilities. In 2022, we went to Lake Poso, located in central Sulawesi, 50 km away from the Palu-Koro fault – the fault that ruptured during the magnitude 7.5 earthquake in Palu in 2018. The goal was to understand the paleoseismology of the region using lake sediments, which act as natural seismographs. During a tremor, the slopes of the lakeshore can be destabilized, causing sediment to collapse. Likewise, active tectonic faults leave their traces in the lake floor with little inundation by erosional processes. Our geophysical instruments can identify these structures, and plant remains from sediment cores allow us to date these events using the radiocarbon dating method. We discovered sedimentary structures indicative of past earthquake shaking and found recurrence approximately every 1,600 years over the last 11,000 years. In addition, we identified an active fault beneath the lake, which we assume can generate a future large-magnitude earthquake.

Keywords: Earthquakes, Bathymetry, Seismic-stratigraphy, Mass-transport deposits, Sulawesi.

1. Introduction

Owing to the convergence of the Pacific, Philippine, Australian, and Eurasian plates, the island of Sulawesi in Indonesia is located in one of the most active tectonic regions in the world (Baillie & Decker, 2022; Hamilton, 1972; Patria et al., 2023; Titu-Eki & Hall, 2020). Most of the convergence is accommodated by a left-lateral strike-slip fault system, including the Palu-Koro Fault (PKF), the Matano Fault, and the Lawanopo Fault between the North Sulawesi Trench and the Tolo Thrust (Figure 1). With an average displacement of 30 mm/year for the PKF (Watkinson & Hall, 2017), the seismic activity is high, as demonstrated by the 2018 Moment Magnitude (Mw) 7.5 Palu earthquake (Frederik, 2019) and several Mw ≥ 6 events along the strike-slip fault trace since 1923 from the International Seismological Centre (ISC) and United States Geological Survey (USGS) instrumental record (Figure 1A). In recent years, several studies have explored Sulawesi's tectonic evolution, fault systems, and the associated seismicity (i.e., Beaudouin et al., 2003; Hall, 2009; Hutchings & Mooney, 2021; Villeneuve et al., 2002). However, the studies predominantly relied on instrumental and historical data and outcrop investigations (Watkinson & Hall, 2017). Only a few events have been instrumentally tracked (ISC and USGS) during the last 60 years (Figure 1B). The instrumental data show seismic activity predominantly along the trace of the Sulawesi strike-slip fault system and adjacent subduction zones with the result that only areas in the vicinity are included in the seismic hazard maps for Sulawesi (Irsyam et al., 2020). Consequently, these records are likely insufficiently long to identify the recurrence pattern of high-magnitude earthquakes, also along other fault systems which may exceed recurrence rates of 100 or 1000 years (Figure 1C).

In presently active seismic zones, such as the Sumatra subduction zone or the Molucca Sea (Hutchings & Mooney, 2021), the recent earthquake catalogue provides a higher probability of better evaluating the hazard potential (Pasari et al., 2021; Supendi et al., 2023), as these regions have demonstrated significant seismic activity during the instrumentally recorded timespan. Areas with absence of significant seismicity during the instrumental period may, however, be temporarily dormant and therefore inadequately represented in hazard potential evaluations posing an underestimated threat (Galli et al., 2019; Rubin & Sieh, 1997; Schulz & Wang, 2014). The Poso Depression region, which is situated in the vicinity of the collision zone where the western and eastern arms of Sulawesi converge, lacks instrumental evidence of large-magnitude earthquakes (Nugraha et al., 2023; Figure 1A and 1B). Within a 200 km radius surrounding the tectonic Poso depression, the occurrence of earthquakes with M > 7 appears to be absent during the past 60 years (Figure 1C). However, the absence of M > 7 events may simply be the result of a return period ≥ 100 years, which is also suggested by extrapolation of the instrumentally recorded events (Figure 1C). Generally, large-magnitude earthquakes (M > 7) often leave traces in outcrops and surface landforms, such as surface ruptures or landslides (Galli et al., 2023; Ocakoğlu & Tuncay, 2023; Tiwari et al., 2021; Waldmann et al., 2011). However, in tropical settings where rainfall is on the order of several meters per year with high surface runoff, substantial weathering, coupled with dense vegetation, causes difficulties in identifying surficially exposed earthquake traces (Bellier et al., 1998). Tectonic lakes, on the contrary, can offer an ideal erosion- and vegetation-free setting where traces of past earthquakes are recorded, either in the form of lake-bottom or subsurface ruptures along active faults as direct proof (on-fault) (Gastineau et al., 2023) or seismically generated sedimentary structures and deposits as indirect evidence of active faulting (off-fault) (Gastineau et al., 2023; Ghazoui et al., 2019; Howarth et al., 2014; Inouchi et al., 1996; Kremer et al., 2017; Moernaut et al., 2007; Schnellmann et al., 2002; Wils et al., 2021). The morphology of the lake floor and subsurface can reveal direct evidence of recent and past tectonic activity. This is expressed in the form of lake bottom offsets, linear fault expressions and pull-apart basins or thrusting and uplift (Fabbri et al., 2021; Lozano et al., 2022; Ribot et al., 2021; Wils et al., 2018). Indirect evidence appears typically in the form of offset linear features such as subaquatic canyon shifts or offsets of submerged paleoshorelines, which allow the delineation of a lateral or vertical displacement of a tectonic lineament lacking surface expression (Alsop et al., 2016; among others). While such primary, on-fault evidence can often be directly linked to an active fault structure, off-fault evidence is typically only indicative of local shaking intensities that are dependent on magnitude, epicentral distance, and local effects. Off-fault evidence becomes more significant when observed at multiple locations independently within the same lake basin or neighbouring sub-basins. Subaquatic mass movements and related turbidites are typical off-fault paleoseismic indicators caused by seismically triggered submerged slope failures (Moernaut et al., 2017). These deposits were successfully used as paleoseismological indicators in many studies worldwide (Adams, 1990; Gràcia et al., 2010; Lu, Moernaut, Bookman, et al., 2021a; Moernaut, 2020). During an earthquake, different locations experience varying amounts of shaking, whereas a Modified Mercalli Intensity (MMI) of ≥ VI is often considered a threshold for inducing slope instabilities (Van Daele et al., 2015). In the case of a high-intensity earthquake, remobilized sediments may occur across large areas of the basin as these can descend the slopes and flow for kilometers driven by density differences, allowing to reach areas far away from their sources, known as hyperpycnal flow (Zavala, 2020). However, subaquatic sediment collapse can be triggered by multiple factors, such as rapid fluctuations in lake level (Anselmetti et al., 2006; Lu et al., 2021b; Tournier et al., 2023; Vogel et al., 2015), excessive precipitation and flooding (Simonneau et al., 2012; Vandekerkhove et al., 2020; Wilhelm et al., 2022), and sediment overload (Hilbe & Anselmetti, 2014; Sabatier et al., 2022). Yet, a seismic source can be suggested when multiple simultaneous

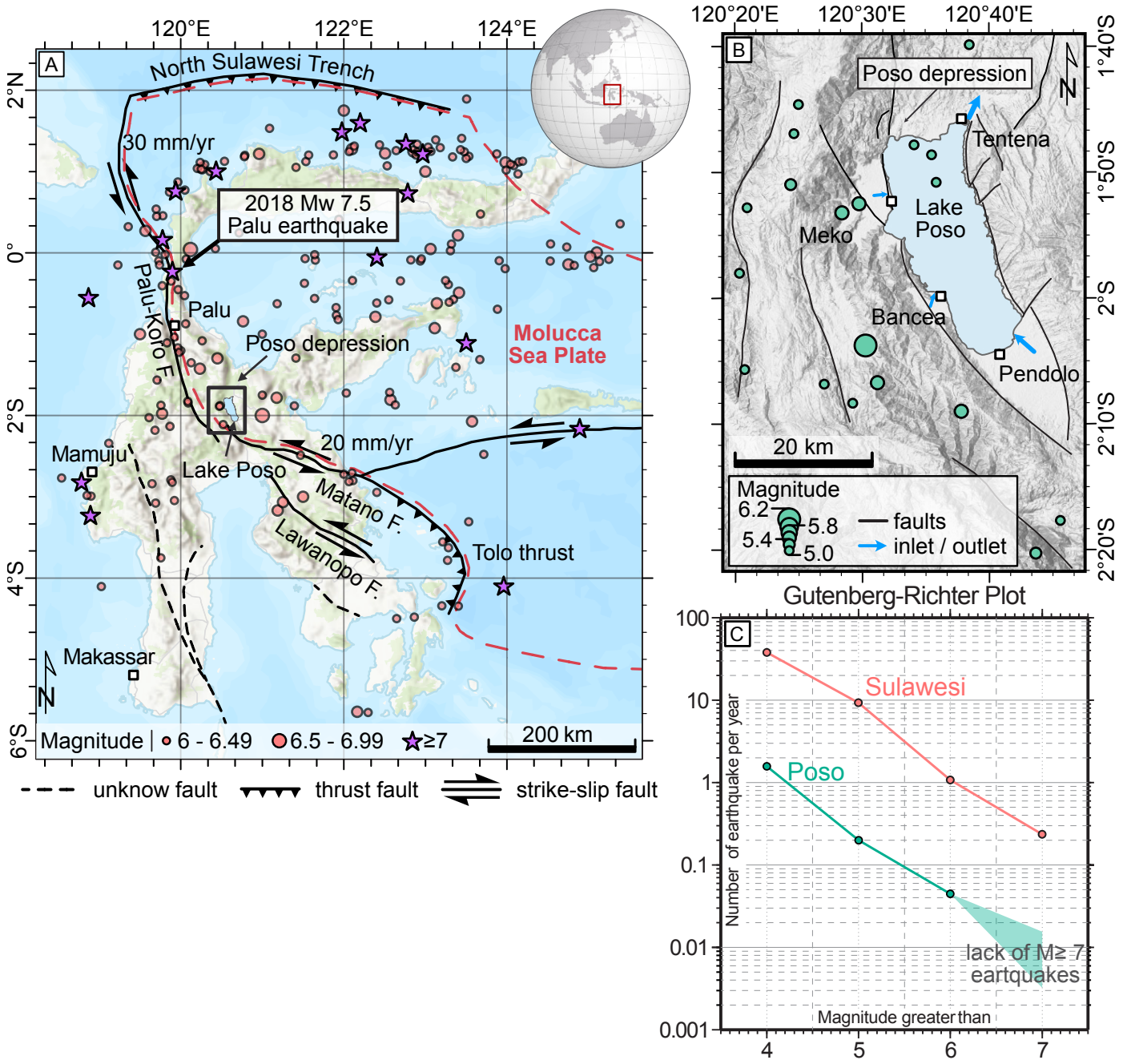

Figure 1 | (A) Tectonic map of the Island of Sulawesi showing earthquakes with a magnitude ≥ 6, depth ≤ 40 km since 1923, documented by USGS and ISC. (B) Seismotectonic map of Lake Poso and its surroundings. (C) Gutenberg-Richter plot illustrating the number of earthquakes per year for Sulawesi (red) and the Lake Poso area (green) based on instrumental records of the last 100 years.

mass wasting events are identified (Schnellmann et al., 2002).

Here, we apply a paleoseismological concept to the tectonic basin of Lake Poso in Central Sulawesi to explore whether large-magnitude earthquakes have occurred in the past. This, in turn, will provide the tools to identify potential hazards in an area that is otherwise designated as a low-hazard zone. For this, we combined detailed multibeam swath bathymetry and seismic reflection data spanning the entire lake area with sediment short cores to provide a thorough characterization of the lake-floor morphology and subsurface sediment architecture. These combined datasets are then used to estimate the evolution of the seismic activity for the Poso Depression while also contributing to the region's seismic hazard awareness.

2. Regional setting

The shape of the island of Sulawesi is a consequence of the collision of the Sula Platform with the northern Australia-New Guinea continental margin. The collision resulted in the rotation of the western volcanic arc and the development of the North Sulawesi Trench (Parkinson, 1998; Silver et al., 1983). Lake Poso (c. 33 km long and c.12 km wide) is elongated in a SSE-NNW direction and formed by the extension of an asymmetric half-graben of the Poso Depression. The half-graben was initially open northwards to the sea, but uplift during the Early Pleistocene bridged east and west Sulawesi, resulting in the closure and disconnection of the basin with the sea (Nugraha et al., 2023). The collision is accommodated by the Sulawesi strike-slip fault system and induced the

obduction of an ophiolite complex to the East (Stevens et al., 1999). The bedrock geology surrounding Lake Poso, therefore, includes a distinct division into two metamorphic units: a mid-Cretaceous metamorphic basement and Mesozoic to Cenozoic phyllites and marble units along the western and eastern shorelines of the lake, respectively (Villeneuve et al., 2002).

Lake Poso is characterized by a humid tropical climate, receiving c. 3,075 mm of annual precipitation (Hidayat, 2019). The lake's major inlets include the Pendolo River to the south and the Meko River to the west, as well as several smaller rivers draining the steeper eastern and northern parts of the catchment (Figure 1B; Damanik et al., 2024). The lake's outlet is formed by the Poso River to the northeast, where it flows through the town of Tentena before draining into the Gulf of Tomini (Figure 1B; Damanik et al., 2024). Nutrient inputs from rivers and anthropogenic land use areas are low, resulting in overall oligotrophic conditions in Lake Poso (Damanik et al., 2024). The water column is presently permanently stratified with bottom-water anoxia and accumulation of redox-sensitive metals and nutrients below the oxycline at c. 90 m water depth (Janssen et al., 2024; Damanik et al., 2024).

3. Material and methods

3.1. Bathymetry acquisition

A 17-day bathymetric survey was conducted on Lake Poso in Nov. 2022, using a Kongsberg EM2040 multibeam echosounder (300 kHz, 1° x 1° beam width) combined with a Leica GX 1230+ GNSS receiver for positioning. The acoustic sound-velocity profiles were measured using a Valeport MiniSVP probe. The bathymetric raw data and the 5 m backscatter mosaics were processed and reviewed using Caris HIPS – SIPS 10.4 software. The maps were generated with ArcGIS pro (v. 3.1.1). The bathymetry point clouds were rasterized using a "swath angle surface" algorithm with a horizontal grid size of 4 m. The raster was interpolated to fill minor data gaps.

3.2. Seismic survey

A seismic acquisition survey was carried out with a single-channel 3.5 kHz Geoacoustic pinger source. A total of 576 km of seismic reflection profiles (Supplementary Figure 1) were recorded to image the lake's subsurface using an independent GPS receiver (Garmin GPS 72H) for positioning. The data were processed with the IHS Markit Kingdom software (v. 2022). To remove noise, a bandpass filter was applied with low-cut and high-cut frequencies of 1500 Hz and 6700 Hz.

3.3. Coring and radiocarbon dating

In addition to the bathymetric and seismic surveys, three short (max. 99 cm long) sediment cores were recovered from the Tentena and Siuri areas, as well as from the depocenter of the lake (Figure 2 for locations) using a UWITEC gravity corer. The UWITEC gravity corer is a typical free-fall corer equipped with steel weights and a plastic liner that is fixed with a ring clamp. Upon entering the sediment, the top of the core liner is closed by a lid to prevent the sediments from falling out on its way back to the surface. The corer is lowered through the water column using a manual winch and low-stretch sailing rope. Depth markings on the rope, along with precise depth information from bathymetric data, are used to estimate the depth from where the corer is released for free fall (c. 3 m above the sediment) after assuring the rope is straight without any noticeable movement. After opening the cores lengthwise, line-scan images were obtained, and a lithological description was performed following standard limnogeological protocols established at the Institute of Geological Sciences of the University of Bern. The cores were sampled every cm and sieved to collect plant macrofossils for radiocarbon dating. Radiocarbon dating was performed on selected plant macrofossils at the Laboratory for the Analysis of Radiocarbon with AMS of the Department of Chemistry at the University of Bern and ETH Zurich. Age-depth models were generated with the Bacon R package v.2.5.8 (Blaauw & Christen, 2011) using the SHCal20 calibration curve. Extrapolation of the sedimentation rates from terminal sediment core depths to deeper target horizons in seismic data is based on a seismic velocity of 1500 m/s and assuming a constant site-specific sedimentation rate.

4. Results

4.1. Lake morphology

With its length of c. 33 km along its SSE-NNW axis, maximum width of 12 km, maximum depth of 395 m, steep slopes (> 20°) along its western and eastern shorelines and more gently dipping slopes (1–4°) to the north and south Lake Poso's morphology is best described as a single tub-shaped basin. The central depocenter is extensive and mostly flat (Figure 2). The bathymetric data of Lake Poso indicate some prominent morphological features: (1) a prominent sinuous and irregular canyon-like structure in the northwestern part of the lake close to the outflow, (2) a confined depression in the northwestern part of the lake, (3) mass transport deposit (MTD) traces, and (4) pockmarks (Figure 2).

4.2. Core description and age model

Short cores were collected from morphologically different areas of the lake to document lithological characteristics and to provide site-specific average sedimentation rates. The core from the depocenter (POS-22-23; 395 m water depth) comprises fine-grained, predominantly siliciclastic sediments interbedded with dark organic matter rich layers interpreted as pelagic background deposits. Sediments appear thinly-bedded between 30–40 cm depth but are interrupted by a c.10 cm thick deposit showing normal

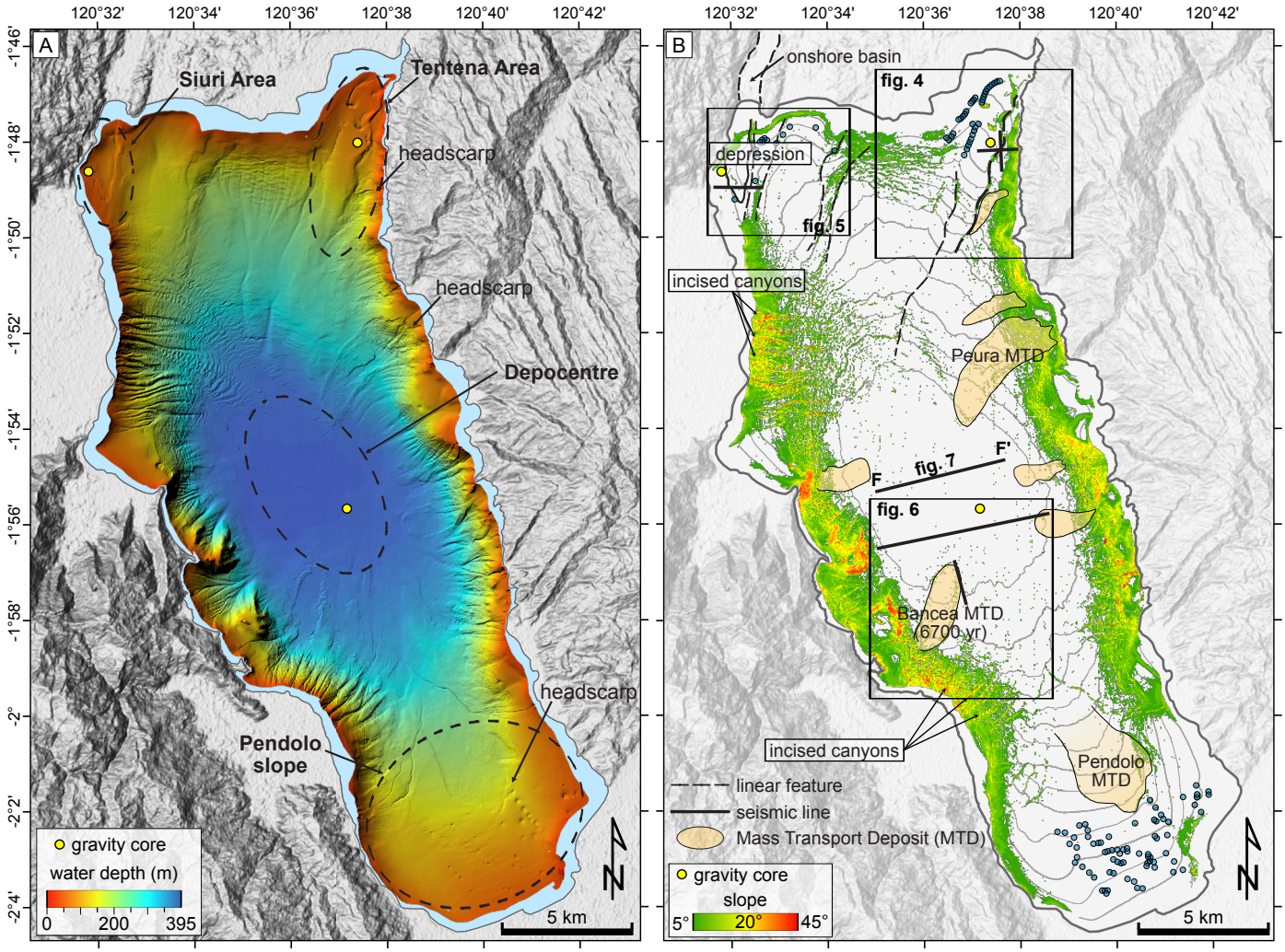

Figure 2 | (A) Bathymetric map of Lake Poso and coring locations discussed here (yellow dots). (B) Interpretation of the bathymetry highlighting the sediment-surface features and the slope-angle map. Blue dots are interpreted as pockmarks, and light-yellow shaded areas are interpreted as mass transport deposits (MTD). Please refer to the Zenodo version of this figure for a Batlow color scale of the bathymetry.

Core ID	Depth (cm)	Type	^{14}C age (year BP)	error	Mean (cal yr BP)	error
POS-22-01	95-96	macrofossil	2168	86	2077	282
POS-22-18	50-51	macrofossil	881	72	784	163
POS-22-23	27-28	macrofossil	348	69	334	149
POS-22-23	45-46	macrofossil	437	65	373	158

Table 1 | Results of AMS ^{14}C-dating

gradation and interpreted as turbidite. Radiocarbon dating from macrofossils retrieved from above and below this deposit suggests turbidite deposition c. 300 cal year BP. The radiocarbon ages suggest sedimentation rates of c. 0.67 mm/year and c. 1.00 mm/year for the sediment above and below the turbidite, respectively. Sediments in the cores from the Tentena (POS-22-01; 79 m water depth) and Siuri sites (POS-22-18; 45 m water depth) to the northeast and northwest, respectively, comprise fine-grained (silty-clay) massive mud and appear slightly reddish in color. Plant macrofossils were retrieved from 95 cm depth in core POS-22-01 (Figure 3; Table 1), revealing a radiocarbon age of c. 2000 cal year BP. This results in an average sedimentation rate of c. 0.44 mm/year for the uppermost sediments. A terrestrial macrofossil retrieved at 50 cm depth in core POS-22-18 (Figure 3) was dated to c. 700 cal year BP, resulting in an average sedimentation rate of c. 0.59 mm/year.

4.3. On-fault evidence in Lake Poso

4.3.1. Tentena area

The bathymetric data show a prominent SW-NE-trending sinuous and irregular canyon-like structure near the outflow in the Tentena area (Figure 4). The offset between the topographic high to the west of the canyon-like structure and its thalweg is c. 20 m (Supplementary Figure 2), extending along longitudinal NW-SE trending sections of up to 280 m in length. Backscatter-intensity data, indicating lake bottom hardness, exhibit extended areas with hard reflectors, interpreted as coarse-grained sediment or

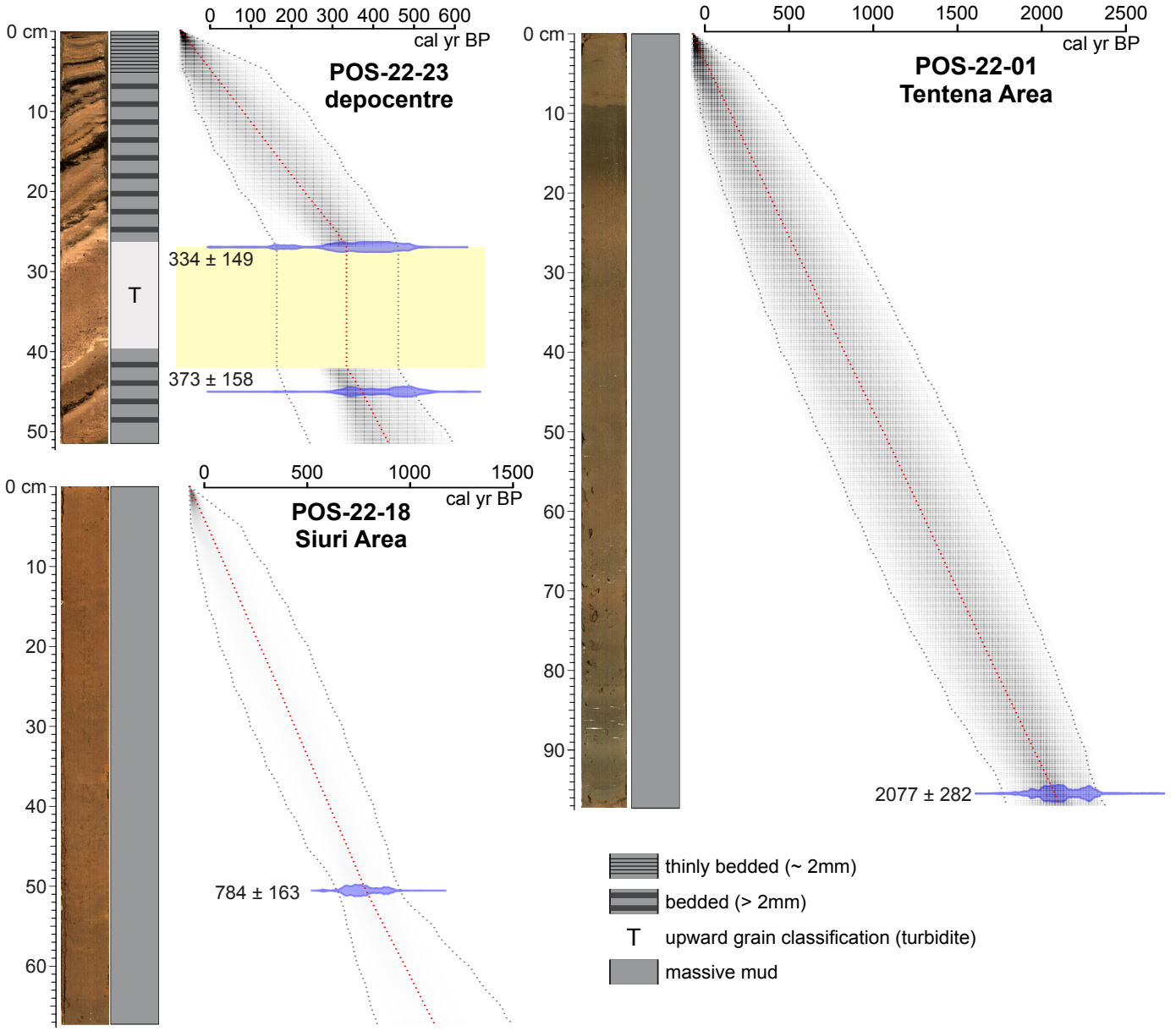

Figure 3 | High-resolution images and simplified lithological description of the cores POS-22-23 (top left; depocenter), POS-22-01 (right; Tentena area) and POS-22-18 (bottom left; Siuri Area) with their respective age-depth models. Dates indicate the mean ± 2SD calibrated age.

outcropping bedrock (indicated in bright yellow in Figure 4B) and dark-blue areas (soft/fine-grained sediments). Moreover, the high backscatter intensity in the Tentena area indicates the presence of hard ground following the sinuous ridge.

Based on the seismic reflection data, we defined two seismic stratigraphic units (Ua below and Ub above) characterized by a similar seismic facies, with a medium-frequency and alternating pattern between high- and low-amplitude reflections (Figure 4). The units are separated by a high-amplitude reflection, marking a sharp angular unconformity, and can be differentiated by the morphology of the reflections. The reflections of Ua are parallel and inclined to the NW (Figure 4D), ending with toplaps at the angular unconformity. Ub is laterally continuous and often fills the irregular surface of the underlying Ua. At the base of the steep slopes, the seismic facies shows medium- to high-amplitude reflections, indicative of a seismic sequence jammed by the bedrock ridge. At greater depth, typically ca. 150 ms two-way travel time (TWT), gas-rich sediments often hamper seismic penetration, preventing imaging of the deeper sections. At the center of the Tentena area, the seismic data shows a large body of acoustically transparent seismic facies, rising vertically from deep sections to the lake floor with almost no sediment cover (Figure 4). In accordance with the high-intensity backscatter signal and the laterally onlapping reflections, this structure is interpreted as a bedrock ridge (Supplementary Figure 2).

Based on the bathymetry and seismic observations, we interpreted the sinuous SE-NW-trending feature with outcropping bedrock as a geomorphic expression of a strike-slip fault with a discernible oblique component. This interpretation is also supported by the SE-NW alignment of pockmarks, delineating secondary faults in the same direction (Figure 2). We attributed the inclined layers within

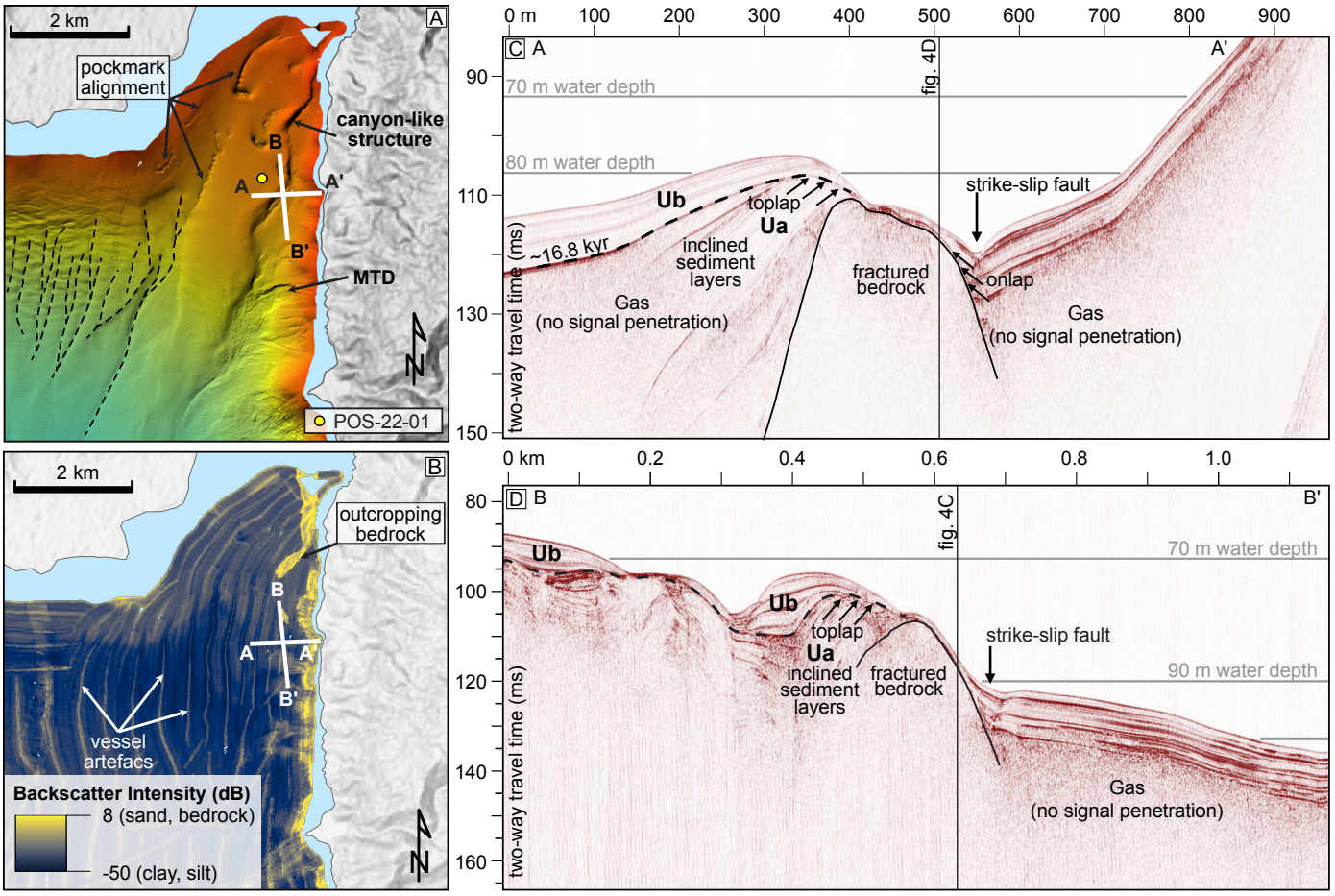

Figure 4 | (A) Bathymetry of the northeastern part of Lake Poso. (B) Backscatter-intensity map. (C) and (D) Seismic reflection profiles crossing the sinusoidal fault trace.

seismic Ua to a tectonic tilting induced by active faulting and bedrock uplift. The overlying and substantially less inclined sediments making up Ub are interpreted as a phase of vertical fault inactivity. Extrapolation of the sedimentation rate of core POS-22-01 (c. 0.44 mm/year) to 10 ms TWT depth (7.5 m of sediment) yields an approximate age of 16.8 kyr for the Ua-Ub boundary.

4.3.2. Siuri area

In the northwestern part of the lake, the lake bottom forms an up to 1 km wide local depression that is bounded by a topographic high to the east, the shoreline to the northwest and a southeast trending ridge along its southwestern extent (Figure 5B). The depression aligns with a basin onshore bounded by a topographic high to the east and a prominent mountain range to the west (Figure 2B). The clearly discernible boundaries of the depression indicate that the feature is the result of active and localized tectonic subsidence bordered by normal faults to the W and E. The seismic data mostly reveal parallel high- and low-amplitude reflections (Figure 5), interpreted as the stratigraphic equivalent of Ub in the northeastern part of the lake. Deeper penetration in the center of the depression is hampered by the presence of gas below c.100 ms TWT (Figure 5). The reflections of Ub are discontinuous near the depression area, where decimetre-scale offsets in the horizons along vertical displacements indicate faults with a normal component (Figure 5C). The fault-related offsets are also discernible as steps on the lake floor, as visible in bathymetric data, indicating recent seismicity.

Seismic profile C–C′ extending basinward from the western shoreline shows a vertical and lateral succession of four stacked clinoform sequences (1–4) below c. 10 m of continuously and acoustically stratified Ub strata. These clinoforms comprise thin horizontal topsets and well-developed foresets, but lack clearly distinguishable bottomsets, except for the topmost clinoform sequence 4, for which a thick bottomset unit can be clearly distinguished in the seismic data. Each individual clinoform sequence is interpreted as a prograding subaqueous delta, with the sequence comprising four vertically distinguishable deltas as the result of significant changes in relative lake level (Marin et al., 2017). Differentiating between tectonic subsidence and climatically driven vertical shoreline changes is not straightforward. Especially in settings controlled by both active tectonics and hydrological changes on similar time-scales, such as Lake Poso.

By extrapolating sedimentation rates (c. 0.59 mm/year) based on a radiocarbon date c. 700 cal year BP for a terrestrial macrofossil retrieved at 50 cm depth in core POS-22-18, (Figure 3), we estimate ages of c. 25 kyr, c. 21.2 kyr and c. 17.5 kyr for the clinoform sequences 2, 3 and 4, respectively. Even when considering the uncertainty of

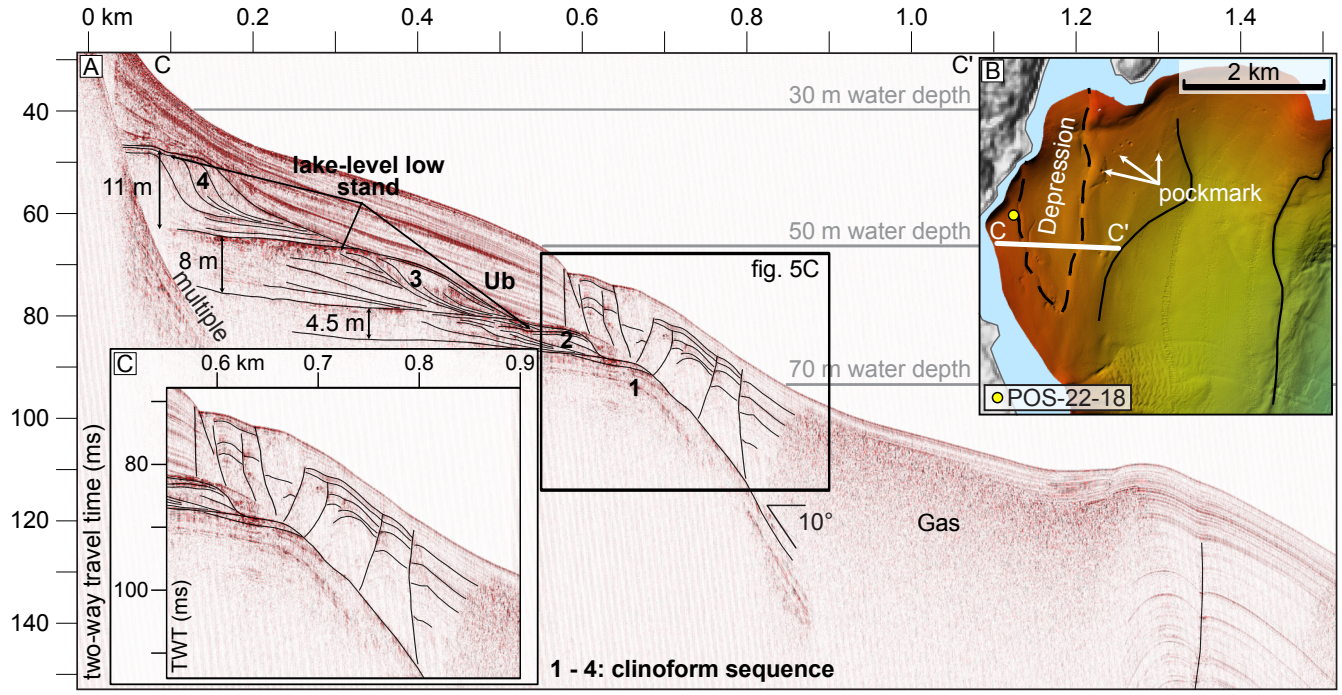

Figure 5 | (A) Seismic reflection line C–C′ crossing the depression in the Siuri Area from W to E (white line in B insert). (B) Bathymetric map of the Siuri area. (C) Zoom on the faults cutting seismic unit Ub to the W. Faults indicating the eastern termination of the depression are indicated by a thin black line in the overview seismic profile.

the sedimentation rates, the ages fall broadly into the Last Glacial Maximum (LGM; 23–18 kyr BP). At nearby Lake Towuti, lake-level indicators (Tournier et al., 2023; Vogel et al., 2015), as well as runoff and dry-adapted vegetation indicators (Russell et al., 2014), suggest a significantly drier regional LGM with up to 30 m lower lake levels. Consequently, we suggest that the clinoform succession likely indicates lake-level lowstands, possibly as a result of a drier than present LGM climate. However, given their location on a slope that seems to align with active faulting with a discernible normal component, we can not completely rule out a tectonic component on relative lake-level changes in this area.

4.4. Off-fault features

We find multiple geomorphic expressions that may serve as tentative off-fault earthquake traces in Lake Poso, comprising mass transport deposits (MTD), turbidites, fluid escapes and pockmarks. Based on their characteristic surface morphologies and distinctive seismic facies, eight large-volume MTDs (> 3 Mm^3) were identified in different parts of Lake Poso (Figure 2). For the most recent MTD, slump head-scarps are clearly visible upslope of the frontally emergent positive topography and the irregular, often blocky surface of the respective MTD. Three MTDs, hereafter named Bancea, Peura and Pendolo (Figure 2), are the result of large-scale substantial slope failures. As is often the case in paleoseismological studies assignment of MTD to earthquakes as a triggering mechanism is difficult. Other triggers, such as heavy rainfall-induced subaerial landsliding, rapid and substantial lake-level changes, gas release, or spontaneous collapses, can also trigger subaquatic slope collapses (Sabatier et al. 2022). However, the size of the deposits, generally low sedimentation rates and the rather rare occurrence of the deposits in combination with the documented frequency of earthquakes generating sufficient intensity in Lake Poso suggest seismic shaking as a plausible trigger mechanism.

Seismic reflection data of lines crossing the MTDs illustrate characteristic acoustically transparent seismic facies with a basal detachment surface and accumulation zones in the center (Figure 6); MTDs are either concave or convex. The internal sedimentary structures are partially well preserved in Lake Poso, as is also reported in other geologically diverse lake settings elsewhere (Frey-Martínez et al., 2006; Gamberi et al., 2011; Sammartini et al., 2021; Strasser et al., 2013). The estimated volumes of the Peura and Pendolo MTDs comprise c. 20 and c. 50 Mm^3, respectively. The Bancea MTD lacks a clearly visible headscarp, and the seismic data coverage is spatially insufficiently resolved for volume calculation. The seismic line E–E′ crossing the depocenter (Figure 6) shows three large units of acoustically transparent facies, with the deepest one associated with the Bancea MTD. Interestingly, this MTD exhibits an unusual topography with a central depression and a topographically higher outer rim (Figure 6A), as was also described for MTDs in Wörthersee, Austria (Daxer et al., 2020), and contrasting with the typical concave-up topography of MTDs (Clare et al., 2019; Moernaut & De Batist, 2011). The seismic line across the Bancea MTD (Figure 6B) shows that the contact between the MTD's transparent seismic facies and the acoustically well-stratified strata, indicating pelagic background sediments, is disrupted along the MTD's outer rim by vertical, chimney-like transparent facies. These vertical chimney-like features with a similar seismic facies as within the

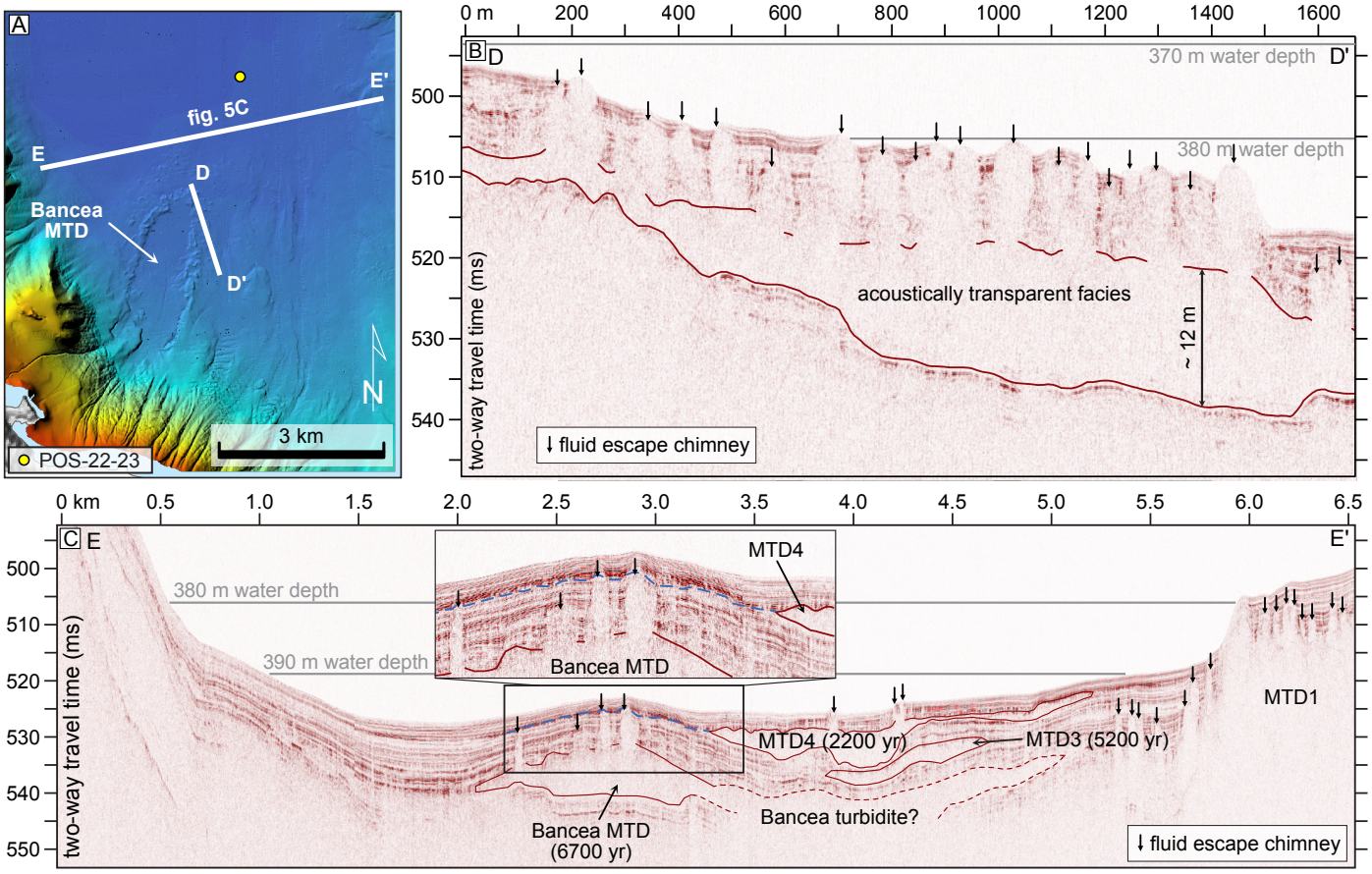

Figure 6 | (A) Magnification of the western slope area and depocenter of the lake, showing the surface expression of a large MTD. (B) Seismic line crossing the terminal part of the Bancea MTD from SSE to NNW showing laterally extensive transparent acoustic facies interpreted as MTD and vertical 'chimney-like' acoustic facies interpreted as fluid escape structures. (C) Seismic line crossing the 395 m deep depocenter from WSW to ENE, a vertically stacked series of transparent acoustic facies interpreted as MTDs.

MTD are interpreted as fluid escape structures that were formed following overloading and dewatering of the under-consolidated and fluid-rich MTD sediment unit. A collapse of the MTD's body accompanied by fluid escapes along its outer rim would explain the peculiar reversed topography of the Bancea MTD. Fluid escape structures related to seismic shaking have also been described in several lakes elsewhere (Moernaut et al., 2009; Praet et al. 2017). Similar, albeit less frequent, fluid-escape structures intersecting the overburden appear on top of other MTDs in Lake Poso (e.g., MTD, Figure 6C), and thus suggesting that these fluid-escape structures represent sediment compaction following compaction and/or seismic shaking. However, it is unclear if every fluid escape structure is the result of variable intensity of different seismic events or due to variable fluid release pressure and volume variations.

Some fluid-escape structures on the Bancea MTD seem to penetrate the overlying sediments but do not propagate through a high-amplitude reflection correlated with the upper MTD4 (Figure 6). This suggests a possible correlation between the fluid escapes and the MTD4's slope-failure event. It remains, however, uncertain whether the fluid escape in the Bancea MTD resulted from seismic shaking triggering the MTD4 event or whether it originated from the impact of the sliding mass. However, the timing of fluid-escape structures on top of the older Bancea MTD, with the emplacement of the MTD4, suggests these fluid escapes could be potential off-fault indicators of earthquakes in Lake Poso.

In addition to these fluid-escape structures associated with the MTDs, pockmarks were identified in the lake floor with the highest spatial densities in both the Tentena area and on the Pendolo slope (Figure 2). While these pockmarks are not always aligned in a systematic manner that would allow correlation with MTDs or fault lineaments in seismic and bathymetric data, they can potentially be associated with seismically triggered fluid escape events (Cojean et al., 2021; Hovland et al., 2002; among others).

Penetration depths of the pinger sonic signal along seismic line F–F' (Figure 7) are restricted to 60 ms TWT in the Siuri area to the W and 20 ms to the E towards the depocenter, resulting in calculated depths of the uppermost c. 45 m and c.15 m, respectively. Six event deposits located in the depocenter (undefined MTDs or turbidites) in the seismic line F–F' (Figure 7) have been identified. These are characterized by a transparent and homogeneous seismic facies, covering large areas with conformable boundaries. Vertical thicknesses of individual event deposits visible in seismic data vary from c. 10 cm (vertical resolution limit of the pinger seismic data) to slightly more than 1 m. Ages of event deposits are rough estimates based on the extrapolation of sedimentation rates from

core POS-22-23, with the deepest visible event deposit 1 dated to c. 11.4 cal kyr BP.

Overall we can identify four MTDs, clearly distinguishable in both seismic and bathymetric data, with roughly estimated ages of c. 11.4 kyr BP (Peura MTD; Figure 7), c. 6.7 kyr BP (Bancea MTD), c. 5.2 kyr BP (MTD3) and c. 2.2 kyr BP (MTD4) (Figure 6). In addition, six MTDs or turbidites visible in seismic line F–F' (Figure 7) crossing the depocenter return age approximations of c. 11.4 kyr BP, c. 6.8 kyr BP, c. 3.2 kyr BP, c. 3.0 cal kyr BP, 2.3 kyr BP and 1.4 kyr BP (Figure 7). The oldest event 1 is likely a turbidite related to the Peura MTD (Supplementary Figure 3).

5. Discussion

Lake Poso shows multiple on- and off-fault indicators for recent and sub-recent seismicity, including active faulting, mass transport deposition, and fluid expulsions (Figure 8). Despite the limitations in terms of the chronological succession of the events observed in our datasets and associated age caveats, we attempt to provide an event stratigraphy and initial interpretations of the observed on- and off-fault features likely associated with pre-historical earthquakes. By combining a rough event stratigraphy framed by the existing chronology with the available instrumental data, we provide a better estimate of possible earthquake magnitude and their recurrence in the Lake Poso region.

The chronostratigraphy of seismic events in Lake Poso (Figure 8) is based on the extrapolation of sedimentation rates derived from the radiocarbon dating of terrestrial plant macrofossils and charcoal found in short sediment cores (Figure 3). Sedimentation rates vary across the entire lake basin, with generally lower sedimentation rates in near-shore areas (c. 0.44 mm/year on core POS-22-01) and highest sedimentation rates in the depocenter (c. 1.00 mm/year on core POS-22-23). Given the abundance of event deposits in the seismic data, we used the bulk sedimentation rate of core POS-22-23 (Figure 3) from the depocenter without prior removal of event deposits for extrapolation purposes. This approach provides a somewhat representative sedimentation rate for extrapolation and age assignment of event deposits and structures visible in seismic reflection data across the depocenter. Additionally, we took the seismic stratigraphy into consideration for extrapolation purposes.

Based on the seismic interpretation and rough age estimates from the extrapolation of sedimentation rates from core POS-22-18, the clinoform sequences 2 (c. 25 kyr BP), 3 (c. 21.2 kyr BP) and 4 (c. 17.5 kyr BP) in the Siuri area are temporarily coincident with the LGM. At nearby Lake Towuti, the LGM is characterized by a drier climate, a more open vegetation cover with abundant C4 grasses, reduced terrestrial runoff (Russell et al., 2014), as well as lower lake levels (Tournier et al., 2023; Vogel et al., 2015). As a result, we suggest that the clinoform successions at Lake Poso are likely morphological features indicative of climate-driven lake-level lowstands, rather than resulting from tectonic activity.

Providing accurate earthquake magnitudes for individual events is challenging based on the available data. However, the observed on-fault features, especially the rupture length of the strike-slip fault in the Tentena Area, can provide a rough estimate for a minimal possible magnitude estimation. The magnitude estimation for the fault in the Tentena area can be calculated using the regression of Mw on surface-rupture length (Stirling et al., 2002) for a pre-instrumental event with the following equation:

$$M_w = a + b \log(L)$$

with Mw being the moment magnitude, a and b the regression parameters (5.89 and 0.79, respectively) and L the fault length in km. For a conservative estimate of the Mw, we only take the section of the fault visible in the bathymetric data with a total length of 7 km into account. When assuming the displacement along the entire length of the fault considered here was produced during a single event, this would result in a minimum Mw of 6.6 ± 0.2. An overestimation of this magnitude is possible, considering that only a small section of the fault could have ruptured. Similarly, if the fault continues onshore beyond the reach

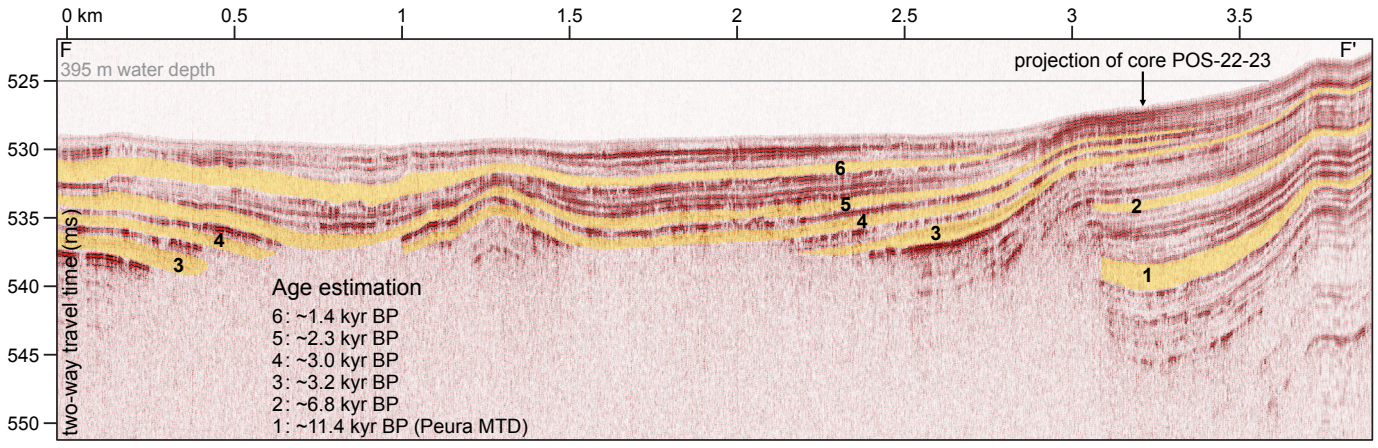

Figure 7 | Seismic line F–F' across the depocenter showing event deposit successions highlighted in yellow, with the estimated ages derived from extrapolation of sedimentation rates of core POS-22-23 retrieved from the depocenter. See Figure 2 for the profile location.

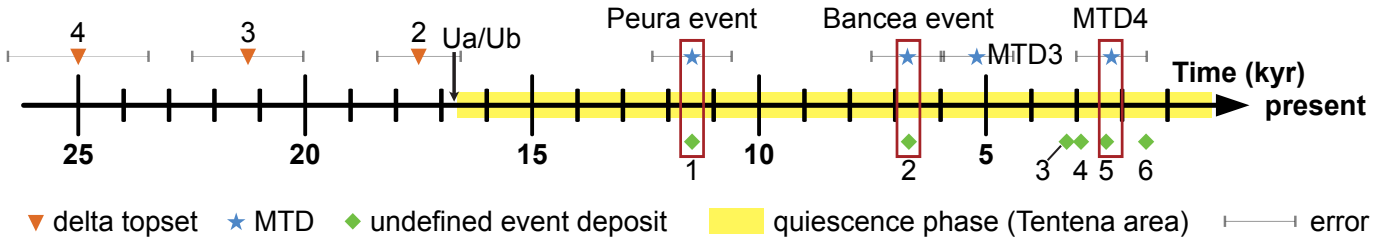

Figure 8 | Time scale representing dated on- and off-fault features and delta topsets in Lake Poso. The red rectangles indicate probable correlations between MTDs and associated turbidites (Figure 6) based on seismic stratigraphic considerations and sedimentation rate extrapolation. The delta topsets (in the Siuri area) are displayed but interpreted to represent climate-induced changes in lake level. They are included here to better visualize the lake's timeline as discussed in the text.

of the bathymetric dataset or offshore, beyond the surface expression of the fault visible in bathymetric data, an underestimation of the magnitude is also possible.

The constructed event catalogue suggests a return period for larger magnitude earthquakes of 1600 ± 1450 years over the last 11 ka only considering the largest MTD. The standard deviation indicates a low confidence in the return period estimation. Nevertheless, the Coefficient of Deviation (CoV) is lower than 1 (CoV = 0.95), which indicates that a weak periodicity prevails, without considering "bursty" data (Salditch et al., 2020). Based on the instrumental record and considering the relationship between the magnitude and the total number of earthquakes in the region, M ≥ 6 earthquakes occur approximately every 55 years (Figure 1). When extrapolating this relationship, M ≥ 7 earthquakes are expected to occur every 1350 ± 450 years, similar to the estimated return period of larger magnitude earthquakes in the proposed Lake Poso event catalogue. The temporal agreement of these return periods suggests that Lake Poso may host a promising paleoseismological archive suitable to record larger magnitude earthquakes. However, additional seismic reflection data allowing for deeper penetration and longer sediment cores are required to refine the age constraints for the event catalogue and to provide a more detailed sedimentological analysis of the event deposits to distinguish seismic from aseismic triggers.

Previous studies show that a minimum intensity of VI is necessary to trigger lacustrine slope failure (Van Daele et al., 2015), depending on the lithology, basin configuration and limnic conditions. Nevertheless, given the different site-specific factors such as sedimentation rates, slope angles, climate and weather conditions, catchment configuration, basin hydrology, and limnological parameters, it is essential to consider the sensitivity of each lake individually to record earthquakes (Wilhelm et al., 2016). Indeed, at nearby Lake Towuti (c. 130 km to the SE of Lake Poso), it is suggested that presently low sedimentation rates in combination with the basin morphology result in a relatively low sensitivity of the lake to record moderate magnitude earthquakes (Tournier et al., 2023; Vogel et al., 2015). Considering the instrumental record, only a single Mw 5.5 earthquake in 2019 with an epicentre distance of c. 3 km from the western lake shore generated intensities > VI (Figure 9). While bathymetric data document fresh surface ruptures with a few decimeters of offsets, there is a lack of evidence for off-fault traces such as subaquatic slope failures related to this event. Conversations with the local population at Lake Poso regarding the 2019 earthquake revealed that the earthquake was strongly noticed and that it generated larger waves washing ashore that day (Herson Rare'a, pers. comm.). Wave generation could be a result of the shaking itself, but may also be related to the subaquatic fault offsets generated close to the western shore visible in seismic data. The lack of recent slope failures that could be related to this event suggests, however, that at Lake Poso, earthquakes with magnitudes larger Mw > 5.5 and intensities > VI are required to trigger mass wasting and consequently that the sensitivity of Lake Poso to record small-magnitude earthquakes is low. This is further supported by the large gap between the number of high-magnitude earthquakes (i.e., one M ≥ 6 earthquake every c. 55 years) and the recurrence of event deposits reported here. In turn, Lake Poso, with its steep slopes along the western and eastern shorelines and overall low near-shore sedimentation rates, is potentially a suitable recorder of primarily strong (Mw > 5.5) local earthquakes with sufficient intensity to trigger slope failure in this setting.

Seismic hazards in near-shore lake settings include tsunami threats (Nigg et al., 2021; Schnellmann et al., 2006). The large MTDs in Lake Poso remobilized large volumes of sediment that likely have the potential to generate tsunami waves. The sediment volumes mobilized during the emplacement of the documented MTDs in Lake Poso suggest a potentially significant tsunami hazard for the town of Tentena and other coastal villages (Supplementary Figure 4). The great depth of the lake, its large volume, and the steep slopes on the eastern and western flanks of the lake basin, which promote corridor long-axis propagation of a tsunami wave, may contribute to further accentuate the propagation of slope failure induced Tsunamis in this setting (Franco et al., 2021).

6. Conclusions

In the tropical setting of seismically active central Sulawesi, where records of pre-historic earthquakes are otherwise scarce, Lake Poso's sediment record has the potential to

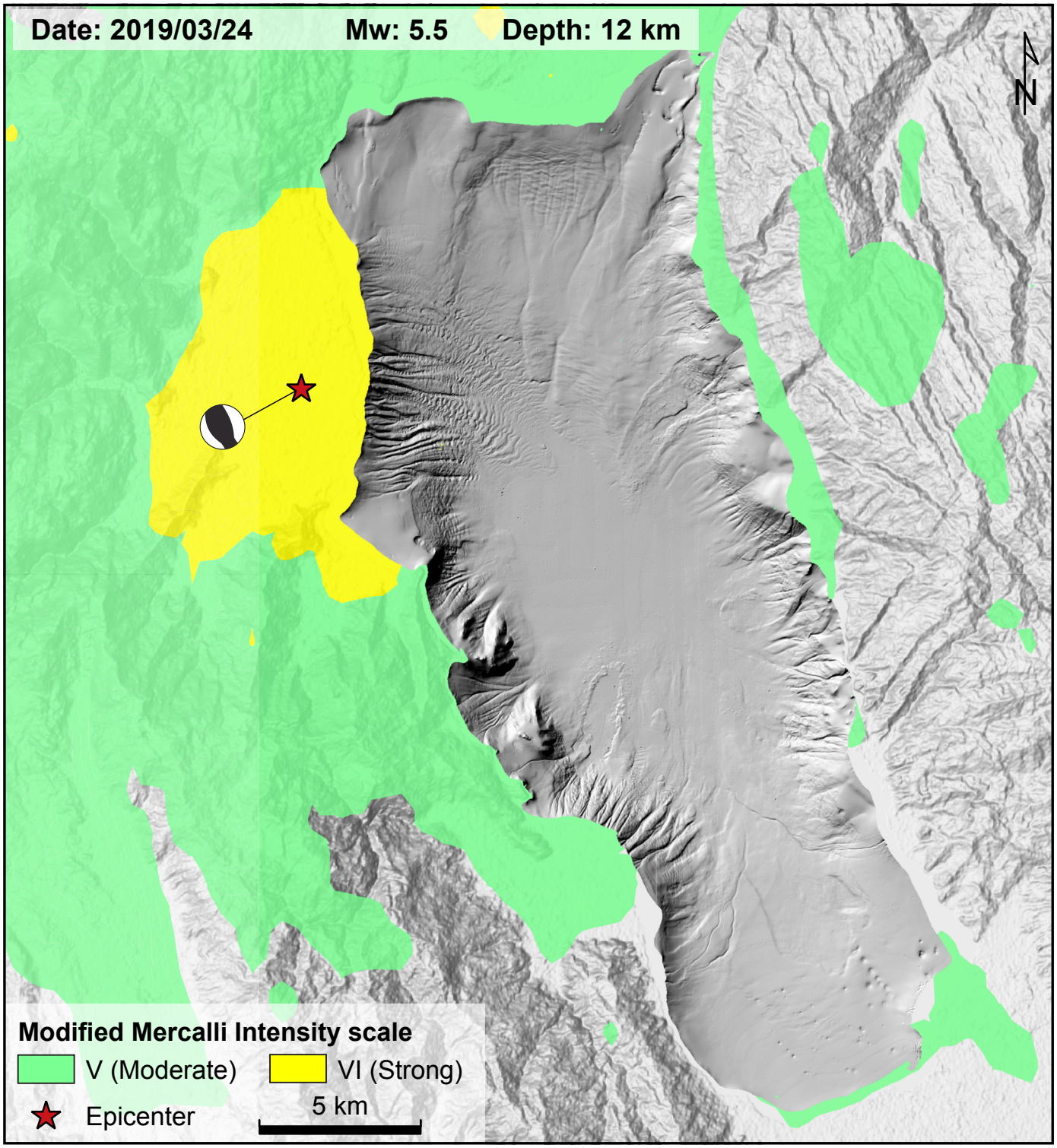

Figure 9 | Intensity (MMI) map of the 2019 Mw 5.5 earthquake located 2 km to the western shoreline of Lake Poso. (USGS Earthquake Hazards Program; https://earthquake.usgs.gov/earthquakes/eventpage/us1000jkv5/shakemap/intensity, modified accessed in Apr. 2024).

provide a valuable archive of past seismic activity. Seismic events in Lake Poso are apparent through characteristic lake-floor morphology features (faults, pockmarks, slide scars) and frequent mass-transport deposits in the subsurface. However, when considering the instrumentally recorded earthquakes in the region and the absence of recent slope failures, we suggest that Lake Poso is rather insensitive to record earthquakes with magnitudes < 5.5 in the form of slope failure induced MTD. Consequently, the inferred event-based return period, albeit based on a so far not robustly constrained chronology, overlaps closely with the expected return period of M ≥ 7 earthquakes based on the Gutenberg-Richter law and the available instrumental record. Considering the chronological uncertainty of the estimated return period of larger magnitude earthquakes and the lack of longer sediment cores allowing for more robust chronological control and sophisticated analysis of the event deposits, these initial data so far provide only a working hypothesis that requires further testing in future studies at Lake Poso.

Owing to the scarcity of paleoseismological studies in lacustrine settings in the tropics, the dataset presented here is considered of an exploratory nature and aimed at motivating more dedicated future studies. The Lake Poso dataset emphasizes the great potential of large tectonic lakes in Indonesia to help fill important knowledge gaps related to past seismic activity in regions where detailed historical and instrumental records are not available and accurate assessment of the seismic hazard is incomplete.

Acknowledgements

This research was carried out with support from the Swiss National Science Foundation, Switzerland (SNSF), through a research grant awarded to H. Vogel (SNSF: 200021_153053). Foreign research permits (43A/SIP/IV/FR/9/2022) for field work at Lake Poso were kindly granted by the National Research and Innovation Agency of Indonesia (BRIN). Many thanks to Herson Rare'a, Marthen Sabintoe and all the locals who contributed to the success of this fieldwork.

Author contribution

NT and HV designed the study with input from SCF and FSA. NT, SCF and HV co-wrote the manuscript with input from all co-authors. NT, AD, SCF, TW, SYC and HV collected data from Lake Poso.

Data availability

The data is available from Zenodo at https://doi.org/10.5281/zenodo.16875260 (Tournier et al., 2025).

Conflict of interest

The authors declare that they have no known competing financial interests or personal relationships that could have appeared to influence the work reported in this paper.

References

Adams, J. (1990). Paleoseismicity of the Cascadia Subduction Zone: Evidence from turbidites off the Oregon-Washington Margin. Tectonics, 9(4), 569–583. https://doi.org/10.1029/TC009i004p00569

Alsop, G. I., Marco, S., Weinberger, R., & Levi, T. (2016). Sedimentary and structural controls on seismogenic slumping within mass transport deposits from the Dead Sea Basin. Sedimentary Geology, 344, 71–90. https://doi.org/10.1016/j.sedgeo.2016.02.019

Anselmetti, F. S., Ariztegui, D., Hodell, D. A., Hillesheim, M. B., Brenner, M., Gilli, A., McKenzie, J. A., & Mueller, A. D. (2006). Late Quaternary climate-induced lake level variations in Lake Petén Itzá, Guatemala, inferred from seismic stratigraphic analysis. Palaeogeography, Palaeoclimatology, Palaeoecology, 230(1–2), 52–69. https://doi.org/10.1016/j.palaeo.2005.06.037

Baillie, P., & Decker, J. (2022). Enigmatic Sulawesi: The tectonic collage. Berita Sedimentologi, 48(1), 1–30. https://doi.org/10.51835/bsed.2022.48.1.388

Beaudouin, T., Bellier, O., & Sebrier, M. (2003). Present-day stress and deformation field within the Sulawesi Island area (Indonesia): Geodynamic implications. Bulletin de La Société Géologique de France, 174(3), 305–317. https://doi.org/10.2113/174.3.305

Bellier, O., Beaudouin, T., Sebrier, M., Villeneuve, M., Bahar, I., Putranto, E., Pratomo, I., Massault, M., & Seward, D. (1998). Active faulting in central Sulawesi (Eastern Indonesia): A geological approch (Scient. Technical Rep. STR Vols 98–14; The GEODYnamics of S and SE Asia (GEODYSSEA), pp. 276–312). Géophysique et Géodynamique Interne - Univ. Paris-Sud Orsay.

Blaauw, M., & Christen, J. A. (2011). Flexible paleoclimate age-depth models using an autoregressive gamma process. Bayesian Analysis, 6(3), 457–474. https://doi.org/10.1214/11-BA618

Clare, M., Chaytor, J., Dabson, O., Gamboa, D., Georgiopoulou, A., Eady, H., Hunt, J., Jackson, C., Katz, O., Krastel, S., León, R., Micallef, A., Moernaut, J., Moriconi, R., Moscardelli, L., Mueller, C., Normandeau, A., Patacci, M., Steventon, M., … Jobe, Z. (2019). A consistent global approach for the morphometric characterization of subaqueous landslides. Geological Society, London, Special Publications, 477(1), 455–477. https://doi.org/10.1144/SP477.15

Cojean, A. N. Y., Kremer, K., Bartosiewicz, M., Fabbri, S. C., Lehmann, M. F., & Wirth, S. B. (2021). Morphology, Formation, and Activity of Three Different Pockmark Systems in Peri-Alpine Lake Thun, Switzerland. Frontiers in Water, 3, 666641. https://doi.org/10.3389/frwa.2021.666641

Damanik, A., Janssen, D. J., Tournier, N., Stelbrink, B., Von Rintelen, T., Haffner, G. D., Cohen, A., Yudawati Cahyarini, S., & Vogel, H. (2024). Perspectives from modern hydrology and hydrochemistry on a lacustrine biodiversity hotspot: Ancient Lake Poso, Central Sulawesi, Indonesia. Journal of Great Lakes Research, 50(3), 102254. https://doi.org/10.1016/j.jglr.2023.102254

Daxer, C., Sammartini, M., Molenaar, A., Piechl, T., Strasser, M., & Moernaut, J. (2020). Morphology and spatio-temporal distribution of lacustrine mass-transport deposits in Wörthersee, Eastern Alps, Austria. Geological Society, London, Special Publications, 500(1), 235–254. https://doi.org/10.1144/SP500-2019-179

Fabbri, S. C., Affentranger, C., Krastel, S., Lindhorst, K., Wessels, M., Madritsch, H., Allenbach, R., Herwegh, M., Heuberger, S., Wielandt-Schuster, U., Pomella, H., Schwestermann, T., & Anselmetti, F. S. (2021). Active Faulting in Lake Constance (Austria, Germany, Switzerland) Unraveled by Multi-Vintage Reflection Seismic Data. Frontiers in Earth Science, 9, 670532. https://doi.org/10.3389/feart.2021.670532

Franco, A., Schneider-Muntau, B., Roberts, N. J., Clague, J. J., & Gems, B. (2021). Geometry-Based Preliminary Quantification of Landslide-Induced Impulse Wave Attenuation in Mountain Lakes. Applied Sciences, 11(24), 11614. https://doi.org/10.3390/app112411614

Frederik, M. C. G. (2019). First Results of a Bathymetric Survey of Palu Bay, Central Sulawesi, Indonesia following the Tsunamigenic Earthquake of 28 September 2018. Pure Appl. Geophys., 176, 14.

Frey-Martínez, J., Cartwright, J., & James, D. (2006). Frontally confined versus frontally emergent submarine landslides: A 3D seismic characterisation. Marine and Petroleum Geology, 23(5), 585–604. https://doi.org/10.1016/j.marpetgeo.2006.04.002

Galli, P., Galderisi, A., Peronace, E., Giaccio, B., Hajdas, I., Messina, P., Pileggi, D., & Polpetta, F. (2019). The Awakening of the Dormant Mount Vettore Fault (2016 Central Italy Earthquake, M

w 6.6): Paleoseismic Clues on Its Millennial Silences. Tectonics, 38(2), 687–705. https://doi.org/10.1029/2018TC005326

Galli, P., Messina, P., Peronace, E., Galderisi, A., Ilardo, I., & Polpetta, F. (2023). Paleoseismic evidence of five magnitude 7 earthquakes on the Norcia fault system in the past 8,000 years (Central Italy). Frontiers in Earth Science, 11, 1188602. https://doi.org/10.3389/feart.2023.1188602

Gamberi, F., Rovere, M., & Marani, M. (2011). Mass-transport complex evolution in a tectonically active margin (Gioia Basin, Southeastern Tyrrhenian Sea). Marine Geology, 279(1–4), 98–110. https://doi.org/10.1016/j.margeo.2010.10.015

Gastineau, R., Sabatier, P., Fabbri, S. C., Anselmetti, F. S., Roeser, P., Findling, N., Şahin, M., Gündüz, S., Arnaud, F., Franz, S. O., Ünsal, N. D., & De Sigoyer, J. (2023). Lateral variations in the signature of earthquake-generated deposits in Lake Iznik, NW Turkey. The Depositional Record, dep2.232. https://doi.org/10.1002/dep2.232

Ghazoui, Z., Bertrand, S., Vanneste, K., Yokoyama, Y., Nomade, J., Gajurel, A. P., & Van Der Beek, P. A. (2019). Potentially large post-1505 AD earthquakes in western Nepal revealed by a lake sediment record. Nature Communications, 10(1), 2258. https://doi.org/10.1038/s41467-019-10093-4

Gràcia, E., Vizcaino, A., Escutia, C., Asioli, A., Rodés, Á., Pallàs, R., Garcia-Orellana, J., Lebreiro, S., & Goldfinger, C. (2010). Holocene earthquake record offshore Portugal (SW Iberia): Testing turbidite paleoseismology in a slow-convergence margin. Quaternary Science Reviews, 29(9–10), 1156–1172. https://doi.org/10.1016/j.quascirev.2010.01.010

Hall, R. (2009). Southeast Asia's changing palaeogeography. Southeast Asia, 54, 14.

Hamilton, W. B. (1972). Tectonics of the Indonesian Region (Report 72–1978; Open-File Report). USGS Publications Warehouse. https://doi.org/10.3133/ofr721978

Hidayat. (2019). Trend of rainfall over Indonesian major lakes from tropical rainfall measuring mission data. IOP Conference Series: Earth and Environmental Science, 303(1), 012019. https://doi.org/10.1088/1755-1315/303/1/012019

Hilbe, M., & Anselmetti, F. S. (2014). Signatures of slope failures and river-delta collapses in a perialpine lake (Lake Lucerne, Switzerland). Sedimentology, 61(7), 1883–1907. https://doi.org/10.1111/sed.12120

Hovland, M., Gardner, J. V., & Judd, A. G. (2002). The significance of pockmarks to understanding fluid flow processes and geohazards. Geofluids, 2(2), 127–136. https://doi.org/10.1046/j.1468-8123.2002.00028.x

Howarth, J. D., Fitzsimons, S. J., Norris, R. J., & Jacobsen, G. E. (2014). Lake sediments record high intensity shaking that provides insight into the location and rupture length of large earthquakes on the Alpine Fault, New Zealand. Earth and Planetary Science Letters, 403, 340–351. https://doi.org/10.1016/j.epsl.2014.07.008

Hutchings, S. J., & Mooney, W. D. (2021). The Seismicity of Indonesia and Tectonic Implications. Geochemistry, Geophysics, Geosystems, 22(9), e2021GC009812. https://doi.org/10.1029/2021GC009812

Inouchi, Y., Kinugasa, Y., Kumon, F., Nakano, S., Yasumatsu, S., & Shiki, T. (1996). Turbidites as records of intense palaeoearthquakes in Lake Biwa, Japan. Sedimentary Geology, 104(1–4), 117–125. https://doi.org/10.1016/0037-0738(95)00124-7

Irsyam, M., Cummins, P. R., Asrurifak, M., Faizal, L., Natawidjaja, D. H., Widiyantoro, S., Meilano, I., Triyoso, W., Rudiyanto, A., Hidayati, S., Ridwan, M., Hanifa, N. R., & Syahbana, A. J. (2020). Development of the 2017 national seismic hazard maps of Indonesia. Earthquake Spectra, 36(1_suppl), 112–136. https://doi.org/10.1177/8755293020951206

Janssen, D. J., Damanik, A., Tournier, N., Tolu, J., Winkel, L., Cahyarini, S. Y., & Vogel, H. (2024). Biogeochemical cycling of trace elements and nutrients in ferruginous waters: Constraints from a deep oligotrophic ancient lake. Limnology and Oceanography, lno.12687. https://doi.org/10.1002/lno.12687

Kremer, K., Wirth, S. B., Reusch, A., Fäh, D., Bellwald, B., Anselmetti, F. S., Girardclos, S., & Strasser, M. (2017). Lake-sediment based paleoseismology: Limitations and perspectives from the Swiss Alps. Quaternary Science Reviews, 168, 1–18. https://doi.org/10.1016/j.quascirev.2017.04.026

Lozano, J. G., Gutierrez, Y. S., Bran, D. M., Lodolo, E., Cerredo, M. E., Tassone, A., & Vilas, J. F. (2022). Structure, seismostratigraphy, and tectonic evolution of Lago Roca (southern Patagonia, Argentina). Geological Journal, 57(8), 3101–3113. https://doi.org/10.1002/gj.4454

Lu, Y., Moernaut, J., Bookman, R., Waldmann, N., Wetzler, N., Agnon, A., Marco, S., Alsop, G. I., Strasser, M., & Hubert-Ferrari, A. (2021a). A New Approach to Constrain the Seismic Origin for Prehistoric Turbidites as Applied to the Dead Sea Basin. Geophysical Research Letters, 48(3). https://doi.org/10.1029/2020GL090947

Lu, Y., Moernaut, J., Waldmann, N., Bookman, R., Alsop, G. I., Hubert-Ferrari, A., Strasser, M., Agnon, A., & Marco, S. (2021b). Orbital- and millennial-scale changes in lake-levels facilitate earthquake-triggered mass failures in the Dead Sea Basin. Geophysical Research Letters, e2021GL093391(n/a), 24. https://doi.org/10.1029/2021GL093391

Marin, D., Escalona, A., Śliwińska, K. K., Nøhr-Hansen, H., & Mordasova, A. (2017). Sequence stratigraphy and lateral variability of Lower Cretaceous clinoforms in the southwestern Barents Sea. AAPG Bulletin, 101(09), 1487–1517. https://doi.org/10.1306/10241616010

Moernaut, J. (2020). Time-dependent recurrence of strong earthquake shaking near plate boundaries: A lake sediment perspective. Earth-Science Reviews, 210, 103344. https://doi.org/10.1016/j.earscirev.2020.103344

Moernaut, J., & De Batist, M. (2011). Frontal emplacement and mobility of sublacustrine landslides: Results from morphometric and seismostratigraphic analysis. Marine Geology, 285(1–4), 29–45. https://doi.org/10.1016/j.margeo.2011.05.001

Moernaut, J., De Batist, M., Charlet, F., Heirman, K., Chapron, E., Pino, M., Brümmer, R., & Urrutia, R. (2007). Giant earthquakes in South-Central Chile revealed by Holocene mass-wasting events in Lake Puyehue. Sedimentary Geology, 195(3–4), 239–256. https://doi.org/10.1016/j.sedgeo.2006.08.005

Moernaut, J., De Batist, M., Heirman, K., Van Daele, M., Pino, M., Brümmer, R., & Urrutia, R. (2009). Fluidization of buried mass-wasting deposits in lake sediments and its relevance for paleoseismology: Results from a reflection seismic study of lakes Villarrica and Calafquén (South-Central Chile). Sedimentary Geology, 213(3–4), 121–135. https://doi.org/10.1016/j.sedgeo.2008.12.002

Moernaut, J., Van Daele, M., Strasser, M., Clare, M. A., Heirman, K., Viel, M., Cardenas, J., Kilian, R., Ladrón de Guevara, B., Pino, M., Urrutia, R., & De Batist, M. (2017). Lacustrine turbidites produced by surficial slope sediment remobilization: A mechanism for continuous and sensitive turbidite paleoseismic records. Marine Geology, 384, 159–176. https://doi.org/10.1016/j.margeo.2015.10.009

Nigg, V., Bacigaluppi, P., Vetsch, D. F., Vogel, H., Kremer, K., & Anselmetti, F. S. (2021). Shallow-Water Tsunami Deposits: Evidence From Sediment Cores and Numerical Wave Propagation of the 1601 CE Lake Lucerne Event. Geochemistry, Geophysics, Geosystems, 22(12), e2021GC009753. https://doi.org/10.1029/2021GC009753

Nugraha, A. M. S., Adhitama, R., Switzer, A. D., & Hall, R. (2023). Plio-Pleistocene sedimentation and palaeogeographic reconstruction in the Poso Depression, Central Sulawesi, Indonesia: From a sea channel to a land bridge. Journal of Palaeogeography, 12(3), 331–357. https://doi.org/10.1016/j.jop.2023.05.003

Ocakoğlu, F., & Tuncay, E. (2023). Geological and geomechanical evidence from the Sünnet landslides (NW Anatolia) for an Mw8.0 cascade rupture in the North Anatolian Fault 8 ky ago. Tectonophysics, 846, 229682. https://doi.org/10.1016/j.tecto.2022.229682

Parkinson, C. (1998). An outline of the petrology, structure and age of the Pompangeo Schist Complex of central Sulawesi, Indonesia. The Island Arc, 7(1–2), 231–245. https://doi.org/10.1046/j.1440-1738.1998.00171.x

Pasari, S., Simanjuntak, A. V. H., Mehta, A., Neha, & Sharma, Y. (2021). A synoptic view of the natural time distribution and contemporary earthquake hazards in Sumatra, Indonesia. Natural Hazards, 108(1), 309–321. https://doi.org/10.1007/s11069-021-04682-0

Patria, A., Natawidjaja, D. H., Daryono, M. R., Hanif, M., Puji, A. R., & Tsutsumi, H. (2023). Tectonic landform and paleoseismic events of the easternmost Matano fault in Sulawesi, Indonesia. Tectonophysics, 852, 229762. https://doi.org/10.1016/j.tecto.2023.229762

Ribot, M., Klinger, Y., Jónsson, S., Avsar, U., Pons-Branchu, E., Matrau, R., & Mallon, F. L. (2021). Active Faults' Geometry in the Gulf of Aqaba, Southern Dead Sea Fault, Illuminated by Multibeam Bathymetric Data. Tectonics, 40(4), e2020TC006443. https://doi.org/10.1029/2020TC006443

Rubin, C. M., & Sieh, K. (1997). Long dormancy, low slip rate, and similar slip-per-event for the Emerson fault, eastern California shear zone. Journal of Geophysical Research: Solid Earth, 102(B7), 15319–15333. https://doi.org/10.1029/97JB00265

Russell, J. M., Vogel, H., Konecky, B. L., Bijaksana, S., Huang, Y., Melles, M., Wattrus, N., Costa, K., & King, J. W. (2014). Glacial forcing of central Indonesian hydroclimate since 60,000 y B.P. Proceedings of the National Academy of Sciences, 111(14), 5100–5105. https://doi.org/10.1073/pnas.1402373111

Sabatier, P., Moernaut, J., Bertrand, S., Van Daele, M., Kremer, K., Chaumillon, E., & Arnaud, F. (2022). A Review of Event Deposits in Lake Sediments. Quaternary, 5(3), 34. https://doi.org/10.3390/quat5030034

Salditch, L., Stein, S., Neely, J., Spencer, B. D., Brooks, E. M., Agnon, A., & Liu, M. (2020). Earthquake supercycles and Long-Term Fault Memory. Tectonophysics, 774, 228289. https://doi.org/10.1016/j.tecto.2019.228289

Sammartini, M., Moernaut, J., Kopf, A., Stegmann, S., Fabbri, S. C., Anselmetti, F. S., & Strasser, M. (2021). Propagation of frontally confined subaqueous landslides: Insights from combining geophysical, sedimentological, and geotechnical analysis. Sedimentary Geology, 416, 105877. https://doi.org/10.1016/j.sedgeo.2021.105877

Schnellmann, M., Anselmetti, F. S., Giardini, D., & Mckenzie, J. A. (2006). 15,000 Years of mass-movement history in Lake Lucerne: Implications for seismic and tsunami hazards. Eclogae Geologicae Helvetiae, 99(3), 409–428. https://doi.org/10.1007/s00015-006-1196-7

Schnellmann, M., Anselmetti, F. S., Giardini, D., McKenzie, J. A., & Ward, S. N. (2002). Prehistoric earthquake history revealed by lacustrine slump deposits. Geology, 30(12), 1131. https://doi.org/10.1130/0091-7613(2002)030<1131:PEHRBL>2.0.CO;2

Schulz, W. H., & Wang, G. (2014). Residual shear strength variability as a primary control on movement of landslides reactivated by earthquake-induced ground motion: Implications for coastal Oregon, U.S.: Strength effects on coseismic landslides. Journal of Geophysical Research: Earth Surface, 119(7), 1617–1635. https://doi.org/10.1002/2014JF003088

Silver, E. A., McCaffrey, R., Joyodiwiryo, Y., & Stevens, S. (1983). Ophiolite emplacement by collision between the Sula Platform and the Sulawesi Island Arc, Indonesia. Journal of Geophysical Research: Solid Earth, 88(B11), 9419–9435. https://doi.org/10.1029/JB088iB11p09419

Simonneau, A., Chapron, E., Vannière, B., Wirth, S. B., Gilli, A., Di Giovanni, C., Anselmetti, F. S., Desmet, M., & Magny, M. (2012). Multidisciplinary distinction of mass-movement and flood-induced deposits in lacustrine environments: Implications for Holocene palaeohydrology and natural hazards (Lake Ledro, Southern Alps, Italy). Climate of the Past Discussions, 8(4), 3205–3249. https://doi.org/10.5194/cpd-8-3205-2012

Stevens, C., McCaffrey, R., Bock, Y., Genrich, J., Endang, Subarya, C., Puntodewo, S. S. O., Fauzi, & Vigny, C. (1999). Rapid rotations about a vertical axis in a collisional setting revealed by the Palu Fault, Sulawesi, Indonesia. Geophysical Research Letters, 26(17), 2677–2680. https://doi.org/10.1029/1999GL008344

Stirling, M., Rhoades, D., Berryman, K., 2002. Comparison of earthquake scaling relations derived from data of the instrumental and preinstrumental era. Bulletin of the Seismological Society of America 92, 812–830.

Strasser, M., Monecke, K., Schnellmann, M., & Anselmetti, F. S. (2013). Lake sediments as natural seismographs: A compiled record of Late Quaternary earthquakes in Central Switzerland and its implication for Alpine deformation. Sedimentology, 60(1), 319–341. https://doi.org/10.1111/sed.12003

Supendi, P., Widiyantoro, S., Rawlinson, N., Yatimantoro, T., Muhari, A., Hanifa, N. R., Gunawan, E., Shiddiqi, H. A., Imran, I., Anugrah, S. D., Daryono, D., Prayitno, B. S., Adi, S. P., Karnawati, D., Faizal, L., & Damanik, R. (2023). On the potential for megathrust earthquakes and tsunamis off the southern coast of West Java and southeast Sumatra, Indonesia. Natural Hazards, 116(1), 1315–1328. https://doi.org/10.1007/s11069-022-05696-y

Titu-Eki, A., & Hall, R. (2020). The Significance of the Banda Sea: Tectonic Deformation Review in Eastern Sulawesi. Indonesian Journal on Geoscience, 7(3), 291–303. https://doi.org/10.17014/ijog.7.3.291-303

Tiwari, P., Maurya, D. M., Shaikh, M., Patidar, A. K., Vanik, N., Padmalal, A., Vasaikar, S., & Chamyal, L. S. (2021). Surface trace of the active Katrol Hill Fault and estimation of paleo-earthquake magnitude for seismic hazard, Western India. Engineering Geology, 295, 106416. https://doi.org/10.1016/j.enggeo.2021.106416

Tournier, N., Fabbri, S. C., Anselmetti, F. S., Cahyarini, S. Y., Bijaksana, S., Wattrus, N., Russell, J. M., & Vogel, H. (2023). Climate-controlled sensitivity of lake sediments to record earthquake-related mass wasting in tropical Lake Towuti during the past 40 kyr. Quaternary Science Reviews, 305, 108015. https://doi.org/10.1016/j.quascirev.2023.108015

Tournier, N. M. B., Fabbri, S. C., Damanik, A., Anselmetti, F., Wiguna, T., Cahyarini, S. Y., & Vogel, H. (2025). Data accompanying the manuscirpt "The large-magnitude earthquake potential of an active strike-slip fault system in Lake Poso, Central Sulawesi, Indonesia" [dataset]. Zenodo. https://doi.org/10.5281/zenodo.16876078

Van Daele, M., Moernaut, J., Doom, L., Boes, E., Fontijn, K., Heirman, K., Vandoorne, W., Hebbeln, D., Pino, M., Urrutia, R., Brümmer, R., & De Batist, M. (2015). A comparison of the sedimentary records of the 1960 and 2010 great Chilean earthquakes in 17 lakes: Implications for quantitative lacustrine palaeoseismology. Sedimentology, 62(5), 1466–1496. https://doi.org/10.1111/sed.12193

Vandekerkhove, E., Van Daele, M., Praet, N., Cnudde, V., Haeussler, P. J., & De Batist, M. (2020). Flood-triggered versus earthquake-triggered turbidites: A sedimentological study in clastic lake sediments (Eklutna Lake, Alaska). Sedimentology, 67(1), 364–389. https://doi.org/10.1111/sed.12646

Villeneuve, M., Gunawan, W., Cornee, J.-J., & Vidal, O. (2002). Geology of the central Sulawesi belt (eastern Indonesia): Constraints for geodynamic models. International Journal of Earth Sciences, 91(3), 524–537. https://doi.org/10.1007/s005310100228

Vogel, H., Russell, J. M., Cahyarini, S. Y., Bijaksana, S., Wattrus, N., Rethemeyer, J., & Melles, M. (2015). Depositional modes and lake-level variability at Lake Towuti, Indonesia, during the past ~29 kyr BP. Journal of Paleolimnology, 54(4), 359–377. https://doi.org/10.1007/s10933-015-9857-z

Waldmann, N., Anselmetti, F. S., Ariztegui, D., Austin Jr, J. A., Pirouz, M., Moy, C. M., & Dunbar, R. (2011). Holocene mass-wasting events in Lago Fagnano, Tierra del Fuego (54°S): Implications for paleoseismicity of the Magallanes-Fagnano transform fault: Holocene mass-wasting events in Lago Fagnano, Tierra del Fuego (54°S). Basin Research, 23(2), 171–190. https://doi.org/10.1111/j.1365-2117.2010.00489.x

Watkinson, I. M., & Hall, R. (2017). Fault systems of the eastern Indonesian triple junction: Evaluation of Quaternary activity and implications for seismic hazards. Geological Society, London, Special Publications, 441(1), 71–120. https://doi.org/10.1144/SP441.8

Wilhelm, B., Amann, B., Corella, J. P., Rapuc, W., Giguet-Covex, C., Merz, B., & Støren, E. (2022). Reconstructing Paleoflood Occurrence and Magnitude from Lake Sediments. Quaternary, 5(1), 9. https://doi.org/10.3390/quat5010009

Wilhelm, Nomade, J., Crouzet, C., Litty, C., Sabatier, P., Belle, S., Rolland, Y., Revel, M., Courboulex, F., Arnaud, F., & Anselmetti, F. S. (2016). Quantified sensitivity of small lake sediments to record historic earthquakes: Implications for paleoseismology: Lake sensitivity to record earthquakes. Journal of Geophysical Research: Earth Surface, 121(1), 2–16. https://doi.org/10.1002/2015JF003644

Wils, K., Deprez, M., Kissel, C., Vervoort, M., Van Daele, M., Daryono, M. R., Cnudde, V., Natawidjaja, D. H., & De Batist, M. (2021). Earthquake doublet revealed by multiple pulses in lacustrine seismo-turbidites. Geology, 49(11), 1301–1306. https://doi.org/10.1130/G48940.1

Wils, K., Van Daele, M., Lastras, G., Kissel, C., Lamy, F., & Siani, G. (2018). Holocene Event Record of Aysén Fjord (Chilean Patagonia): An Interplay of Volcanic Eruptions and Crustal and Megathrust Earthquakes. Journal of Geophysical Research: Solid Earth, 123(1), 324–343. https://doi.org/10.1002/2017JB014573

Zavala, C. (2020). Hyperpycnal (over density) flows and deposits. Journal of Palaeogeography, 9(1), 17. https://doi.org/10.1186/s42501-020-00065-x

How to cite: Tournier, N., Fabbri, S., Damanik, A., Anselmetti, F., Wiguna, T., Cahyarini, S. Y., & Vogel, H. (2025). The large-magnitude earthquake potential of an active strike-slip fault system in Lake Poso, Central Sulawesi, Indonesia . Sedimentologika, 3(1). https://doi.org/10.57035/journals/sdk.2025.e31.1604